



# Enhancing the thermal and crystallization properties of polypropylene through carbon nanotube integration: a comprehensive investigation

Maziyar Sabet<sup>1</sup>

Received: 22 September 2023 / Accepted: 16 December 2023 / Published online: 2 March 2024  
© Iran Polymer and Petrochemical Institute 2024

## Abstract

The present investigation focuses on elucidating the novel impact of both carbon nanotubes (CNTs) and multi-walled carbon nanotubes (MWCNTs) on thermal behavior and crystallization kinetics of isotactic polypropylene (PP) composites. Our primary objective is to unveil the distinctive influence of these nanotubes on PP crystallization and its thermal properties, paving the way for tailored applications in high-performance materials. Incorporating CNTs led to a noteworthy elevation in crystallization temperature without significantly altering the polymer melting point. Furthermore, our findings revealed an increased critical cooling rate in correlation with higher CNT concentrations, representing a crucial parameter for nucleation effectiveness, independent of CNT load and crystallization temperature. The study demonstrated CNTs' specific role in expediting the  $\alpha$ -phase development in PP during isothermal crystallization experiments. Additionally, the investigation into MWCNTs within PP nanocomposites highlighted a pivotal percolation threshold at 0.5% (by weight) MWCNTs. Below this threshold, enhancements in physical properties were observed without requiring a compatibilizer. Augmented interfacial area between PP and MWCNTs notably enhanced PP's thermal stability, particularly evident at elevated temperatures, with heat-treated fibers exhibiting a distinct, narrow melting peak at 170 °C. These novel discoveries significantly advance our understanding of how CNTs impact PP crystallization and underscore the development of superior PP nanocomposites endowed with heightened thermal properties, catering to targeted applications demanding superior performance.

**Keywords** Thermal properties · Crystallization procedure · Carbon nanotubes · Multiwall carbon nanotubes · Polypropylene · Nanocomposite

## Introduction

Carbon nanotubes (CNTs) exhibit remarkable tensile strength and modulus, situated as ideal nano-reinforcements in polymer matrices [1–3]. Their extensive aspect ratios, low densities, and high specific areas [4–6] make CNTs effective in carrying loads, owing to both their excellent aspect ratios and electrical conductivity [7–9]. The interaction between CNTs and the polymer matrix influences the capacity of polymer chains to envelop CNT surfaces which may impact the contact resistance of CNTs [10–12]. Despite extensive studies on semi-crystalline polymers and CNTs, limited attention has been given to the implications of polymer

crystallization on electrical characteristics [13–15]. Recent research suggests that CNTs, due to their propensity to form crystals with semi-crystalline polymers, are enveloped in a thick trans-crystalline layer of polymer crystals [16–18]. Depending on synthesis conditions, CNTs can be single-walled or multi-walled (MWCNT) and exhibit extraordinary mechanical properties, including a tensile modulus of 1 TPa, tensile strength of 11–63 MPa, and compressive strength of 150 GPa [22–24]. The high aspect ratio of CNTs allows their introduction in minimal quantities while significantly enhancing the physical characteristics of polymer materials [25–27]. Incorporating CNTs into polymer matrices enhances mechanical characteristics and the glass transition temperature ( $T_g$ ) [28–30]. Polypropylene (PP), a common semi-crystalline polymer, exists in various crystalline forms, including the monoclinic  $\alpha$ -phase and the disordered structure mesophase [31–33]. Extensive studies on MWCNT-reinforced PP reveal that nanotubes serve as  $\alpha$ -phase nucleation agents [34–36]. Macromolecules partially wrapped

✉ Maziyar Sabet  
maziyar.sabet@utb.edu.bn

<sup>1</sup> Petroleum and Chemical Engineering, Universiti Teknologi Brunei (UTB), Jalan Tungku Link, Mukim Gadong A, Bandar Seri Begawan BE1410, Brunei Darussalam

around CNTs, oriented parallel to them, can act as nuclei for folding crystals [37–39]. Crystallization studies of high-surface polymers, including PP, have employed fast scanning calorimetry and nucleation agents [40–42]. In the industrial sector, polymer-based materials, particularly polyolefins like PP, are favored for their lightweight nature, chemical resistance, ease of processing, and recyclability [42]. The incorporation of carbon-based nanomaterials, such as CNTs and MWCNTs, has shown promise in enhancing polymer nanocomposite properties [43]. However, challenges arise in dispersing CNTs or MWCNTs within the polymer matrix due to their propensity for aggregation [44]. Strategies, such as grafting reactive moieties onto PP and optimizing processing techniques, have been explored to improve dispersion and compatibility [45, 46]. Studies on PP/MWCNT nanocomposites demonstrate improvements in mechanical properties [47]. Nevertheless, excessive amounts of CNTs or MWCNTs can lead to agglomeration and a subsequent decline in mechanical performance [48]. Optimizing CNT or MWCNT content is crucial to maximize benefits while mitigating the negative effects of agglomeration [49]. Ongoing research focuses on surface modification and processing techniques to overcome these challenges and enhance the mechanical characteristics of PP/CNTs or PP/MWCNTs nanocomposites [50]. In conclusion, CNTs hold significant potential as nano reinforcements in polymer matrices, offering exceptional characteristics even in small quantities. The careful optimization of CNT content is essential to prevent agglomeration and maximize the benefits of CNT incorporation. Surface modification and processing techniques are being explored to address dispersion challenges and further enhance the mechanical characteristics of PP/CNTs or PP/MWCNTs nanocomposites [1–3].

This study aimed to investigate the influence of CNTs on the thermal and crystallization characteristics of PP composites. Utilizing melt processing techniques, including extrusion and injection molding, PP/CNT and PP/MWCNT nanocomposites were fabricated with MWCNT loadings ranging from 0 to 1.0% (by weight). The research tests were conducted non-isothermal and isothermal crystallization using differential scanning calorimetry (DSC) to assess how CNTs affected PP crystallization under different supercooling conditions. Nucleation efficacy, representing the efficiency of CNTs as nucleating agents, was evaluated based on critical cooling speed in non-isothermal studies. The study explored the impact of CNTs on the crystalline state of isotactic PP, derived a nucleation efficiency parameter from the critical cooling speed and nanotube content, and validated the reinforcement effect of CNTs through dynamic mechanical analysis. Results indicated that CNTs accelerated the development of the  $\alpha$ -phase in isothermal crystallization experiments, with composite fiber shrinkage less than 5%. The melting point of PP and its nanocomposites ranged between

150 and 152 °C, with crystallinity varying based on CNT content. The research further examined the influence of different quantities of MWCNTs on the thermal properties of PP/MWCNT composites, with a specific focus on excluding potential chemical interactions. Comprehensive microstructural examinations of PP/MWCNT composites were conducted, analyzing various thermal characteristics and comparing them to existing literature results. The practical implications of this study include the potential for developing improved materials with enhanced physical properties, such as increased thermal stability and reduced shrinkage. Percolation threshold is the minimum concentration of a conductive filler in a composite material at which a continuous conductive network is formed. In the case of CNT-reinforced PP composites, a percolation threshold was observed at 0.5% (by weight) of MWCNTs. Below this threshold, the physical properties of the composites improved without the need for a compatibilizer. The percolation threshold is important for both thermal and electrical conductivities. It indicates the point at which the conductive filler particles are in close enough proximity to form a continuous pathway for heat or electricity to flow through the material. In the case of PP nanocomposites with MWCNTs, the percolation threshold at 0.5% (by weight) MWCNTs led to an enhancement in PP thermal stability and improved thermal properties [4–6]. The identified percolation threshold can serve as a guideline for determining the optimal amount of MWCNTs in PP nanocomposites. There are many research aspects in this field such as: (i) development of superior PP nanocomposite materials with enhanced thermal properties, (ii) potential for improved materials with increased thermal stability and reduced shrinkage, (iii) enhancement of the mechanical properties of PP nanocomposites, such as tensile strength and modulus, (iv) application potentials in industries that require lightweight materials with chemical resistance, ease of processing, and recyclability, (v) possibility of using CNTs as nanoreinforcements in polymer matrices, offering exceptional characteristics even in small quantities, (vi) optimization of CNT content to prevent agglomeration and maximize the benefits of CNT incorporation, and (vii) exploration of surface modification and processing techniques to address dispersion challenges and further enhance the mechanical characteristics of PP-CNT nanocomposites. However, the findings contribute to the understanding of the impact of carbon nanotubes on PP crystallization and the development of improved PP nanocomposite materials with enhanced thermal and mechanical properties. These materials have potential applications in various industries that require lightweight, chemically resistant, and thermally stable materials. This study aims to comprehensively investigate and elucidate the effects of CNTs and MWCNTs on the thermal characteristics and crystallization process of PP composites. Specifically, the objectives are as follows:

- Derivation of a nucleation effective parameter to quantitatively assess the impact of varying CNT loads and crystallization temperatures on crystalline structure and nucleation behavior of PP composites.
- Examination of the influence of CNTs on the enhancement of  $\alpha$ -phase crystalline structure in PP, analyzing their role in altering the crystallization kinetics and thermal stability of the material.
- Validation of the reinforcement effect of CNTs within PP matrices through comprehensive dynamic mechanical analysis, aiming to understand the mechanical enhancements and temperature-dependent behavior attributed to CNT inclusion.
- Investigating the impact of different quantities of MWCNTs on the thermal properties of PP-MWCNT composites, focusing on elucidating the effects while excluding potential chemical interactions between the nanotubes and the polymer matrix.
- Contribution to an in-depth understanding of how MWCNTs influence the behavior and properties of PP nanocomposites, providing valuable insights and knowledge for designing and optimizing materials tailored for diverse and specific applications across various industries.

## Experimental

### Materials

The composite utilized the PP matrix Novolen 1106H from Lyondell Basell Industries, which is characterized by a melt flow index (MFI) of 2.2 g/(10 min) at 2.16 kg and 230 °C, a density of 0.913 g/cm<sup>3</sup>, and molecular weight parameters ( $M_w$  462 kg/mol,  $M_n$  85 kg/mol). This specific type of PP was chosen due to its anticipated absence of nucleating agents and its predominant isotactic nature, with a tacticity of 93.9%.

To facilitate the preparation process, the granular material was transformed into a 0.5–1 mm-sized powder using liquid nitrogen. The CNTs and MWCNTs employed in the composite were Nanocyl™ NC7000, manufactured by Nanocyl S.A. in Belgium, exhibiting a mean diameter and length of 9.5 nm and 1.5  $\mu$ m, respectively. Prior to incorporation, the nanotubes underwent vacuum drying at 120 °C for one hour. Mechanical premixing of the PP matrix and MWCNTs took place at ambient temperature, laying the foundation for subsequent processing steps.

### Preparation of PP composites

The preparation of PP/CNT or MWCNT nanocomposite specimens involved a two-step blending procedure. In the

initial stage, PP-MWCNT pellets were generated using a co-rotating twin-screw extruder. The extruder operated at a screw velocity of 330 rpm, and the barrel temperature increased progressively from the main feeder to the die, maintaining a temperature range of 155–205 °C. Subsequently, the nanocomposite pellets were shaped into 4 mm-thick plates for mechanical testing. The process employed an injection molding device, with the barrel temperature held within the range of 210–235 °C and the mold temperature set at 35 °C. Control parameters for injection pressure and rate were established at 89 bar and 45 rpm, respectively. To explore the impact of varying nanotube loading levels on material characteristics, nanofillers were introduced in nanocomposite compositions ranging from 0 to 1.0% (by weight). These compositions underwent further processing into sheets with different thicknesses using a calendaring process. This facilitated the shaping and formation of the final composite materials.

### Characterization

The thermal stability of the samples was assessed through thermogravimetric analysis (TGA) utilizing a TA Instruments Q500 instrument. The analysis involved subjecting the samples to a heating ramp from room temperature to 800 °C at a rate of 20 °C/min. Two distinct environments, air and nitrogen (N<sub>2</sub>) were employed for the measurements. Open ceramic pans, each containing samples weighing approximately 10 mg, were utilized. In the air environment, a constant heating rate of 10 K/min was applied with a gas flow of 20 mL/min. The resulting thermographs were meticulously examined to ascertain crucial parameters such as the melting temperature, melting enthalpy, and oxidation temperature of the samples. For the investigation of blending and crystallization performance in both pure PP and the nanocomposites, a heat flux DSC, the ExStar 6200 by SII Nanotechnology, was employed. The equipment underwent calibration using enhanced purity calibration standards like indium, tin, and zinc metals to ensure precise temperature and heat flow readings. During the DSC analyses, specimens weighing approximately 8–11 mg were placed in an aluminum crucible. The samples underwent a heating rate of 10 °C/min, starting from 0 to reaching 230 °C. Subsequently, the specimens were held at this temperature for 2 min to eliminate any thermal history. To cool the specimens from 230 to 0 °C, an electrical cooling instrument, the Thermo Scientific EK90C/SII intra cooler, was employed at a cooling rate of 10 °C/min. This cooling process was crucial to facilitate the melt-crystallization process. After completing the melt-crystallization procedure, the specimens were maintained at 0 °C for an additional 2 min. Following this, the specimens were reheated from 0 to 230 °C using a

heating rate of 10 °C/min. Throughout the entire experiment, a nitrogen (N<sub>2</sub>) atmosphere was maintained with a flow rate of 50 mL/min to prevent any thermal degradation of the specimens. To determine the degree of crystallinity (X<sub>c</sub>%) for the nanocomposites, Eq. 1 was applied as part of the calculation process. The degree of crystallinity serves as a metric for the crystalline portion within the material, providing essential insights into the thermal characteristics of the nanocomposites.

$$X_c(\%) = \frac{\Delta H_m}{\Delta H_m^\circ(1-\alpha)} \times 100 \quad (1)$$

In Eq. 1, the nanocomposite crystallinity rate (X<sub>c</sub>%) is calculated based on several factors. ΔH<sub>m</sub> represents the second melting enthalpy quantity of the sample, measured in joules per gram (J/g), obtained through experimentation. The term (1−α) denotes the weight percentage of PP in the specimen. Additionally, ΔH<sub>m</sub><sup>°</sup> represents the enthalpy quantity of melting for a 100% crystalline form of PP, established at 209 J/g, as referenced in [42–44]. Through the application of these experimental techniques and calculations, a comprehensive examination of both pure PP and composites' melting and crystallization behaviors was conducted, yielding valuable insights into their thermal properties. A thermomechanical analyzer (TMA) (Q400, TA Instruments) was utilized to quantify fiber shrinkage. This involved heating a 10-filament bundle at an average speed of 5 °C/min from ambient temperature to 170 °C, maintaining a tension of approximately 3.2 MPa. The size of the fibers used for TMA testing can vary depending on the specific experimental requirements and instrument capabilities. In the case of a 10-filament bundle sample, the fibers are preferably bundled together to form a larger composite sample for analysis, potentially resulting in a total sample size in the range of 5 mm in diameter and 3 cm in length. Dynamic mechanical analysis (DMA) measurements were performed on test specimens with dimensions of 20 × 8 × 1 mm<sup>3</sup>. Conducted in tensile mode using a Q800 instrument from TA Instruments, USA, this analysis aimed to characterize the T<sub>g</sub> of the nanocomposites within the temperature range of −40 to 100 °C. Measurements employed a frequency of 1.0 rad/s, and the heating rate was set to 3 K/min. For the examination of fractured surfaces of the PP/MWCNT nanocomposite, scanning electron microscopic (SEM) photos were captured. A thin layer of gold was sputter deposited onto the specimens before imaging to enhance conductivity and provide a clear imaging surface. Imaging was conducted under elevated vacuum conditions using Nano SEM 650 equipment operating at 5 kV. This analysis facilitated the visualization and characterization of the morphology, offering insights into filler-matrix interactions and the

overall composite structure. X-ray diffraction (XRD) patterns were obtained using a Siemens D500 diffractometer equipped with CuKα radiation (wavelength λ = 0.154 nm). Measurements covered the 2θ range from 6° to 56°, with a step size of 0.04° and a counting time of 5 s. XRD analysis enabled the determination of the nanocomposite material's crystalline structure and phase composition, providing valuable information on the distribution and alignment of MWCNTs within the matrix. Raman spectra were acquired using a Perkin-Elmer GX Fourier Transform spectrometer. The excitation source was a diode-pumped Nd: YAG laser operating at 1065 nm. Spectra were collected in the spectral span of 90–3400 cm<sup>−1</sup>, offering information about vibrational modes and molecular structure. For each spectrum, 1000 images were combined to enhance the signal-to-noise ratio. Raman spectroscopy provided insights into the nanocomposite's vibrational characteristics and molecular structure Figs. 1 and 2.

## Results and discussion

The thermal stability of both PP/CNT and PP/MWCNT composites was investigated through TGA analysis, revealing the influence of CNT content. In the context of PP/CNT composites, the incorporation of 0.5% (by weight) CNTs notably enhances the thermal stability of the PP matrix. This enhancement is evident in a degradation temperature of 340 °C, surpassing that of pure PP by 22 °C. TGA diagrams illustrate a substantial improvement in thermal stability, with a minimum increase of 50 °C observed when 1% (by weight) of CNTs or MWCNTs was introduced. The initiation temperature of degradation sees a significant rise of over 75 and 105 °C in the presence of CNTs and MWCNTs, respectively,

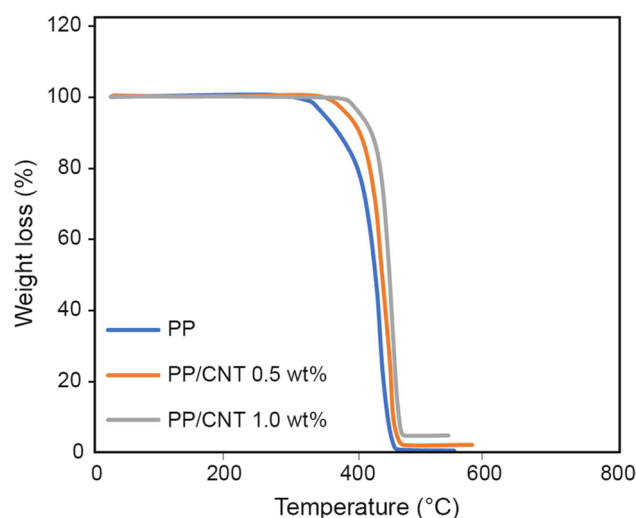
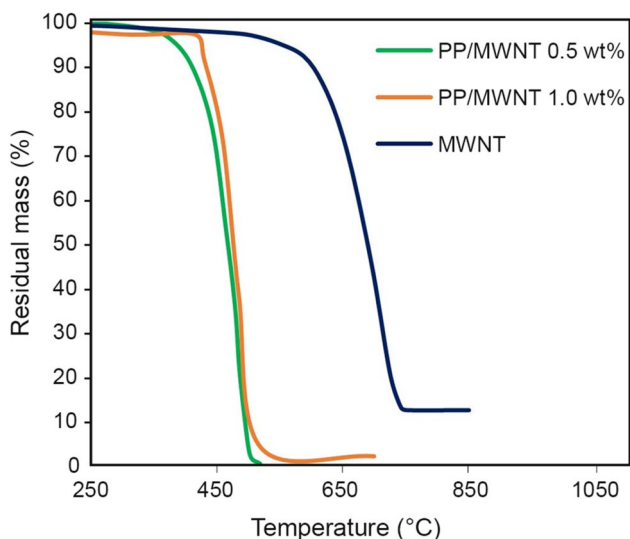


Fig. 1 Weight loss results of pristine PP and PP/CNT composites



**Fig. 2** Weight loss results of PP, MWCNT, and PP/MWCNT composites

indicating a noteworthy enhancement in thermal stability [1–3]. Further augmentation of CNT content to 1% (by weight) results in an additional improvement, marked by a shift in the onset temperature to 445 °C. The presence of CNTs fosters the generation of a higher residue or char post-degradation, contributing to the preservation of composite structural integrity at elevated temperatures. Similarly, in the case of PP/MWCNT composites, the addition of 0.5% (by weight) MWCNTs enhances the thermal stability of the PP matrix. This improvement is evidenced by a reduced rate of mass loss and an elevated temperature at which the peak mass loss occurs during the degradation process. The larger surface area provided by MWCNTs fosters increased interactions with the polymer matrix, leading to a discernible enhancement in thermal stability. Mechanistically, this improvement is attributed to the effective quenching of free radicals by MWCNTs and the physical adsorption of PP chains onto the surfaces of MWCNTs [4–6]. In comparison, both types of composites exhibit superior thermal stability when contrasted with pure PP. The incorporation of CNTs and MWCNTs elevates the degradation temperature and promotes the formation of a protective residue or char post-degradation. This enhancement in thermal stability is noticeable even with a 0.5% (by weight) addition of both CNTs and MWCNTs. However, concerning specific quantities, the PP/CNT composite displays a higher degradation temperature of 350 °C compared to the PP/MWCNT composite. The latter exhibits a reduced rate of mass loss and a higher temperature at the peak mass loss, indicating distinct characteristics and interactions of CNTs and MWCNTs with the polymer matrix. In summary, the incorporation of both CNTs and MWCNTs significantly boosts the thermal stability of the

PP matrix, as evidenced by the specific quantities and values derived from the TGA analysis. However, to comprehensively grasp the underlying mechanisms and optimize CNT and MWCNT compositions for optimal thermal stability in PP composites, further in-depth studies are imperative [7–9].

Figures 3, 4, 5 and 6 illustrate the outcomes of DSC tests performed on both pristine PP and PP/CNT composites to probe their thermal characteristics. DSC, a technique measuring heat flow during thermal transitions, was employed to discern key parameters such as melting temperature ( $T_m$ ) and crystallization temperature ( $T_c$ ) [10–12]. Notably, pure PP exhibited a singular peak at 117.2 °C for  $T_c$ . However,  $T_c$  exhibited an incremental trend with rising CNT concentrations in the PP/CNT composites. The introduction of 0.5%

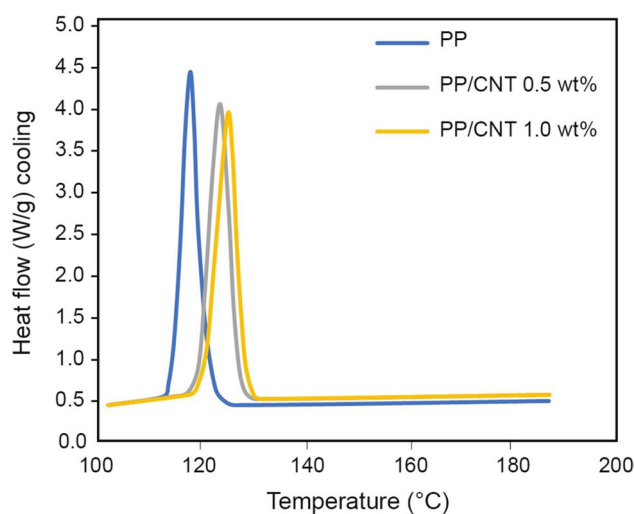


**Fig. 3** Heat flow (cooling) of pristine PP and PP/CNT composites

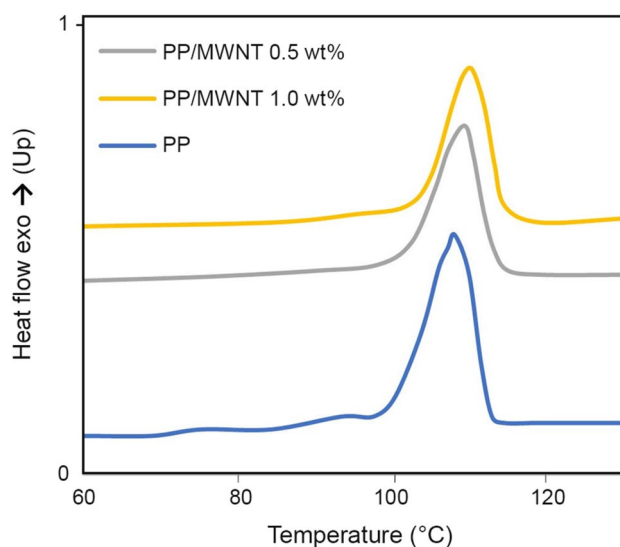


**Fig. 4** Heat flow (exothermic) of PP, and PP/MWCNT composites



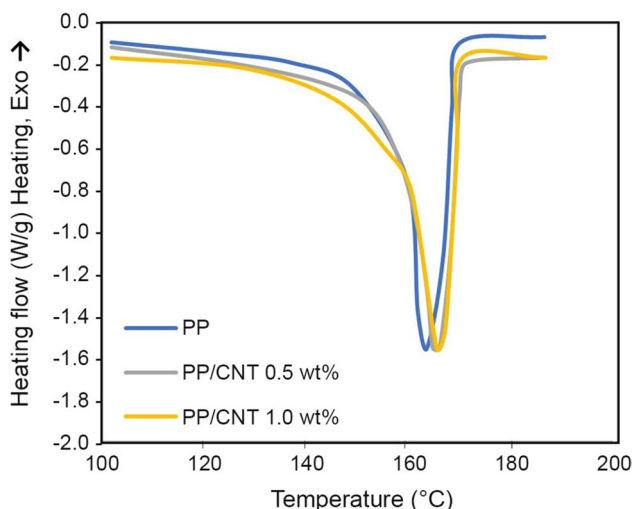


**Fig. 5** Heat flow (heating) of pristine PP and PP/CNT composites

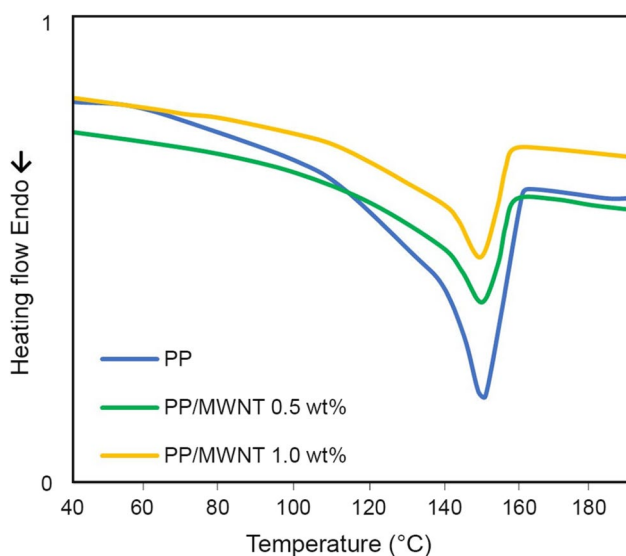


**Fig. 6** Heat flow (endothermic) of PP, and PP/MWCNT composites

(by weight) CNTs led to a 10 °C elevation in  $T_c$ , with further increases observed at higher CNT contents. Surprisingly, the DSC findings indicated that the presence of CNTs did not influence the melting behavior or  $T_m$  of PP; both PP and its

nanocomposites exhibited melting temperatures within the range of 150 to 152 °C. The degree of crystallinity ( $X_c\%$ ) in the nanocomposites, however, demonstrated variation based on CNT content. Conversely, the inclusion of MWCNTs showcased an enhancement in the crystallization behavior of PP, evident through elevated crystallization temperatures and enthalpy values compared to pure PP. The impact of MWCNTs on  $X_c\%$  is correlated with the quantity of CNTs or MWCNTs incorporated into the PP matrix. Table 1 details how the addition of CNTs or MWCNTs alters crucial parameters, including melting temperature, heat of melting, degree of crystallinity, glassy transition temperature, and crystallization temperature, for both pristine PP and PP composites. Moreover, the DSC data hinted at a minimal influence on lamellar thickness, melting temperature, and crystallinity due to varying MWCNT quantities. In summary, the DSC analysis revealed that CNTs, particularly MWCNTs, served as nucleating agents, enhancing the crystallization behavior of PP. The increase in  $T_c$  of the nanocomposites paralleled the ascending CNT content, while the  $T_m$  of both PP and its nanocomposites remained constant.  $X_c\%$  exhibited a rise up to 0.5% (by weight) of MWCNTs, followed by a slight decline at higher concentrations. These findings are in line with prior studies and underscore the significance of comprehending the impact of nanoparticles on polymer crystallization to establish meaningful structure–property relationships. The dispersion quality of MWCNTs significantly influenced the crystallization characteristics of PP, whereas the melting behavior ( $T_m$ ) of PP was minimally affected by the addition of MWCNTs [13–15].

The non-isothermal crystallization behavior of both pristine PP and PP/CNT composites was investigated in relation to cooling rate and CNT content. Figure 7 illustrates the non-isothermal crystallization characteristics of pristine PP and composites with 0.5% and 1.0% CNT content. The presence of CNTs affected the crystallization temperature, which varied with the CNT content. Higher CNT content significantly impacted the composite crystallization behavior [16–18]. Faster cooling rates resulted in shorter crystallization times, higher nucleation speeds, and an elevated maximum crystallization temperature. Conversely, slower cooling rates provided more time for crystal growth, leading to a lower maximum crystallization temperature. Higher

**Table 1** Melting temperature, heat of melting, degree of crystallinity, glassy transition temperature and crystallization temperature for pristine PP and PP composites

Sample	Melting				Crystallization $T_c$ (°C)
	$T_m$ (°C)	$\Delta H_f$ (J/g)	$X_c$ (%)	$T_g$ (°C)	
PP	162.7	98.3	47.2	−4.5	117.3
PP/CNT0.5% (by weight)	164.0	100.5	48.4	−4.6	127.5
PP/CNT1.0% (by weight)	164.8	107.4	51.9	−4.9	128.2
PP/MWCNT 0.5% (by weight)	162.9	99.5	47.9	−4.6	119.5
PP/MWCNT 1.0% (by weight)	163.1	99.1	47.6	−4.7	121.4

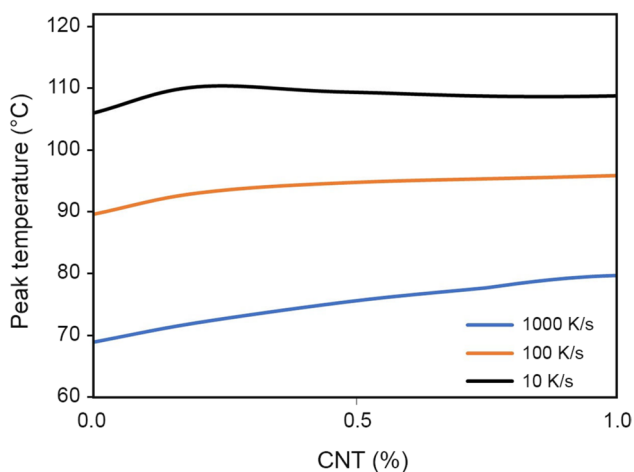


**Fig. 7** Peak temperature alterations at various cooling rates of pristine PP and PP/CNT composites

cooling rates correlated with an increase in the maximum temperature of the crystallization peak, suggesting that the crystallization process occurred at a higher temperature. Notably, a higher CNT content (1.0%) induced distinct crystallization kinetics and potentially altered the maximum temperature of the crystallization peak under various cooling rates. These insights shed light on the impact of CNTs on the crystallization process, contributing to our understanding of nucleation, growth mechanisms, and thermal behavior for optimization purposes. The experimental results, detailed in Table 1, demonstrate that the addition of CNTs enhanced the crystalline level ( $X_c$ ) of pure PP by 1.0% (from 47.1 to 51.9% by weight). However, further increases in CNT content did not accelerate the crystallization of the composites. CNTs played a dual role in PP crystallization: acting as nucleating agents that promoted crystalline structure formation in the PP matrix, leading to increased crystalline levels with lower CNT amounts, and simultaneously restricting PP chain mobility, limiting access to crystallization sites, and impeding further crystallization with higher CNT concentrations. This intricate interplay between CNTs and PP during crystallization highlights both positive and negative effects on PP's crystallization behavior. The  $T_g$  is a critical factor when utilizing amorphous polymers for specific applications, determining the transition between glassy/crystalline and rubbery physical properties. In this study, polymer samples with varying concentrations of MWCNTs were examined. The mechanism for crystallization in carbon nanotube-reinforced polypropylene Composites are explained as the introduction of CNTs into PP composites led to an elevation in crystallization temperature and an increase in the critical cooling speed, indicating the influence of CNT concentration and cooling rate on the crystallization process. A nucleation effectiveness parameter was

devised to assess the impact of CNT load and crystallization temperature on PP composites, providing insights into the nucleation mechanism. CNTs specifically expedited the development of the  $\alpha$ -phase crystalline structure in PP, contributing to the enhanced thermal stability of the nanocomposites. The addition of CNTs and MWCNTs to the PP matrix improved the storage modulus and mechanical characteristics of the composites, indicating a reinforcing effect. The XRD analysis revealed that the addition of MWCNTs promoted the formation of the b-crystalline phase in PP-MWCNT composites, potentially enhancing mechanical properties and thermal stability. Figure 7 presents the outcomes of a DSC investigation, illustrating how MWCNTs influence  $T_g$ . At low MWCNT contents (up to 0.5% wt), there was an increase in  $T_g$  compared to the neat polymer. This suggests that MWCNTs influenced the polymer's crystallization behavior, potentially acting as nucleation sites for ordered structure formation. The accelerated crystallization process resulted in a higher  $T_g$ . The observed increase in  $T_g$  at low MWCNT concentrations can be attributed to the uniform reinforcement provided by MWCNTs, restricting polymer chain mobility and reducing amorphous regions. However, beyond a certain threshold, the effect of MWCNT concentration on  $T_g$  may change, depending on the system and the interaction between the polymer and MWCNTs. In general, MWCNTs at low concentrations exhibited a reinforcing effect, raising  $T_g$  and improving the mechanical properties of PP composite for challenging conditions. The addition of CNTs influences the crystallization behavior of the PP matrix [19–21]. Specifically, it leads to an increase in crystallization temperature without significantly altering the melting point of PP. The presence of CNTs acts as nucleating agents, enhancing the crystallization process by promoting the formation of a more ordered crystalline structure within the PP matrix. However, the melting point of PP remains relatively unchanged, indicating that while CNTs affect the crystallization kinetics, they do not significantly impact the temperature at which PP transitions from solid to liquid [1–3].

Figures 8 and 9 illustrate the outcomes of DMA conducted on PP/CNT composites, showcasing essential parameters and values. Figure 8 also shows the substantial difference in storage modulus at  $-200$  °C between using CNT and MWCNT despite the same reinforcement percentage can be attributed to the inherent structural disparities between CNT and MWCNT. MWCNTs possess a higher aspect ratio and greater interfacial area, promoting stronger interactions with the polymer matrix [22–24]. This results in improved load transfer and enhanced reinforcement capabilities, leading to a notably higher storage modulus compared to CNTs, even at equivalent reinforcement percentages. The storage modulus in both PP/CNT and PP/MWCNT composites surpasses that of pure PP, particularly at elevated temperatures,

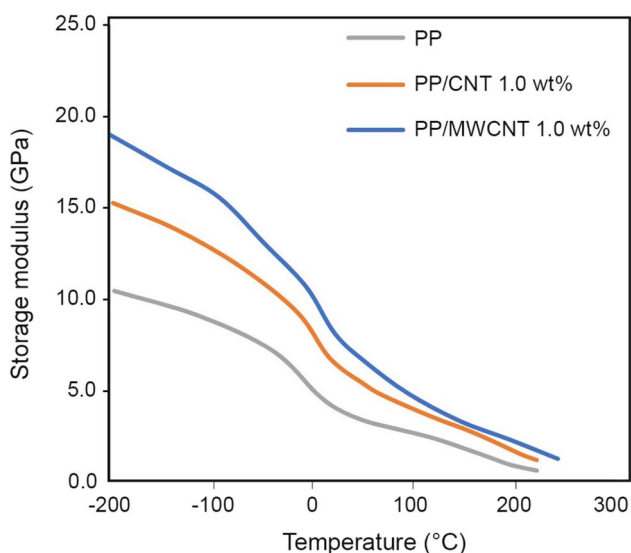


**Fig. 8** Storage modulus of PP, and PP composites at various temperatures

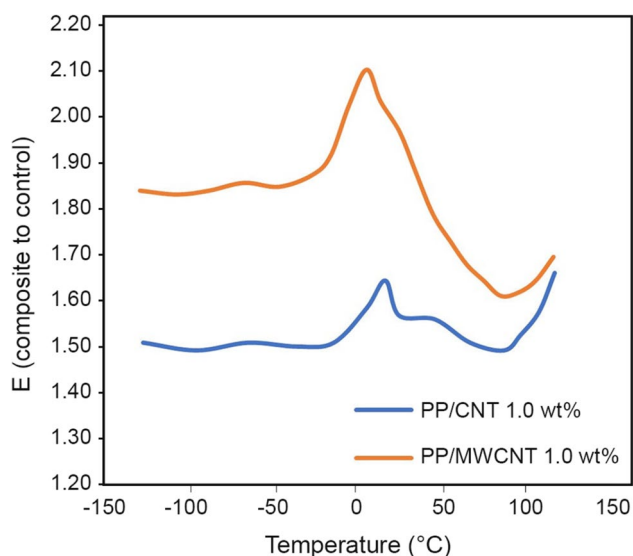


**Fig. 10** Storage moduli ratios of PP/CNT and PP/MWCNT (1.0% by weight) at various temperatures

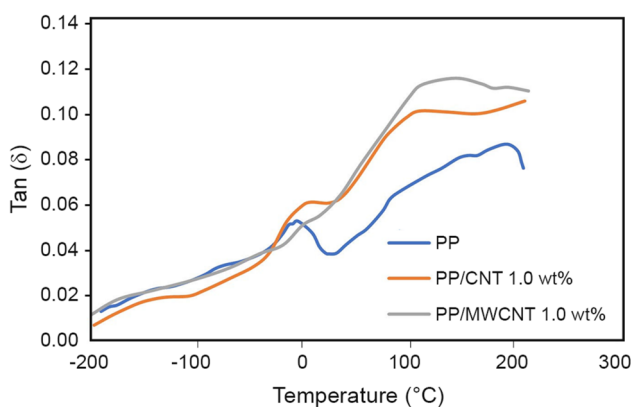


**Fig. 9** Loss tangent of PP, and PP composites at various temperatures

indicating the reinforcing influence of CNTs and MWCNTs. The incorporation of CNTs or MWCNTs holds the potential to enhance the  $T_g$  of the composites by restricting the mobility of PP chains. The robust interfacial connection between the PP matrix and carbon nanotubes, coupled with the "labyrinth effect" and thermal insulation properties, collectively contribute to the heightened thermal stability of these nanocomposites. The  $\text{Tan}(\delta)$  peak, representing energy dissipation, shifts to higher temperatures in the presence of both CNTs and MWCNTs.

Figures 10 and 11 present the storage modulus ratios and differences at various temperatures, providing insights into the temperature-dependent mechanical behavior of PP composites. The addition of carbon nanotubes amplifies the storage modulus, augments the weight loss degree, improves thermal stability, and shifts the  $\text{Tan}(\delta)$  peak to

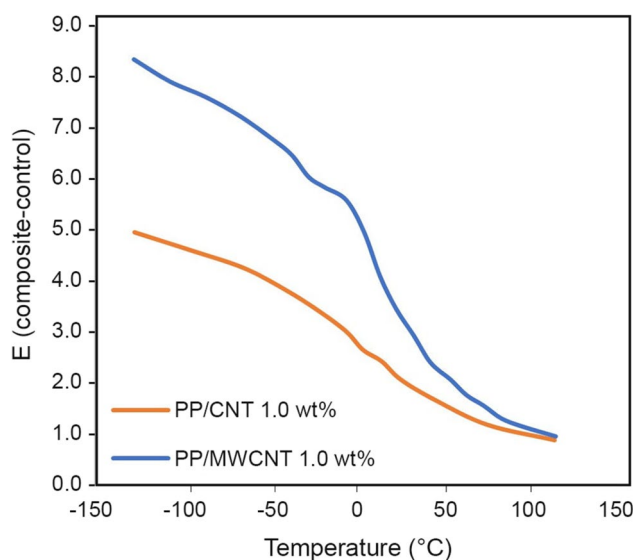


**Fig. 11** Storage moduli differences of PP/CNT and PP/MWCNT (1.0% by weight) at various temperatures

higher temperatures. However, it is noteworthy that the  $T_g$  of the nanocomposites experiences a reduction compared to pure PP. The robust interfacial association between the polymer matrix and CNTs or MWCNTs, in conjunction with the labyrinth effect, significantly contributes to the enhanced thermal stability observed in these composites [25–27].

In this investigation, we scrutinized the shrinkage behavior and thermal expansion characteristics of pristine PP and PP/CNT composites across various temperatures, as illustrated in Fig. 12, to assess their dimensional stability and thermal properties. The findings revealed that, at a specific



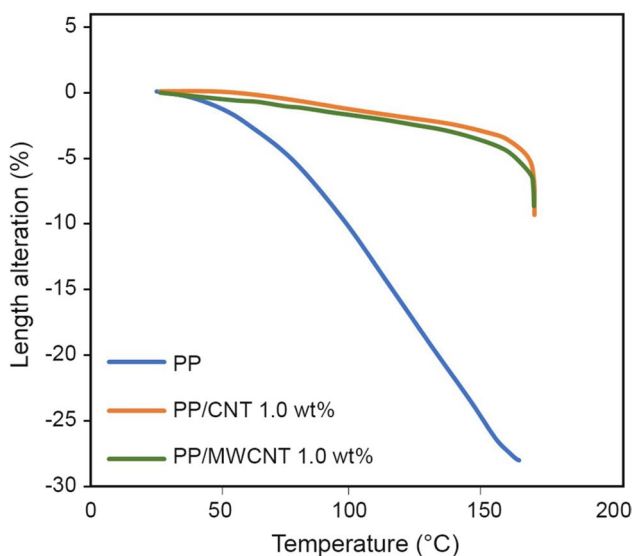


**Fig. 12** Shrinkage results of PP and PP composites at various temperatures

temperature, all composite fibers exhibited less than 5% shrinkage, while pristine PP experienced a notable 27% shrinkage at 160 °C. Intriguingly, even at low concentrations of 0.5% or 1.0% (by weight), the inclusion of CNTs in the composites led to a remarkable reduction in shrinkage, suggesting a robust interaction between PP and CNTs. Additionally, we investigated the thermal expansion behavior of the materials. Both pristine PP and PP/CNT composites exhibited thermal expansion at elevated temperatures. However, the presence of CNTs influenced the thermal expansion characteristics, with higher CNT concentrations resulting in modified thermal expansion behavior compared to pristine PP. To evaluate the thermal stability and suitability for high-temperature applications, we specifically examined the shrinkage behavior of the PP/MWCNT 1.0% (by weight) composite. The outcomes demonstrated that the degree of shrinkage in the composite was less than 5% at the specified temperature. This substantial reduction in shrinkage, even at a low nanotube concentration, indicates the reinforcing effect of MWCNTs in restricting the movement of polymer chains and enhancing dimensional stability [31–33]. The robust interface between the MWCNTs and the polymer matrix further supports this observation, suggesting effective dispersion of the nanotubes in PP without additional treatments. Quantitatively comparing the data, while pristine PP exhibited a shrinkage of approximately 27% at 160 °C, all composite fibers, including the PP/MWCNT 1.0% (by weight) composite, showed shrinkage of less than 5% at the same temperature. This underscores the efficacy of incorporating CNTs in mitigating the shrinkage behavior of the composites. Furthermore, the inclusion of CNTs at low concentrations significantly altered the thermal expansion

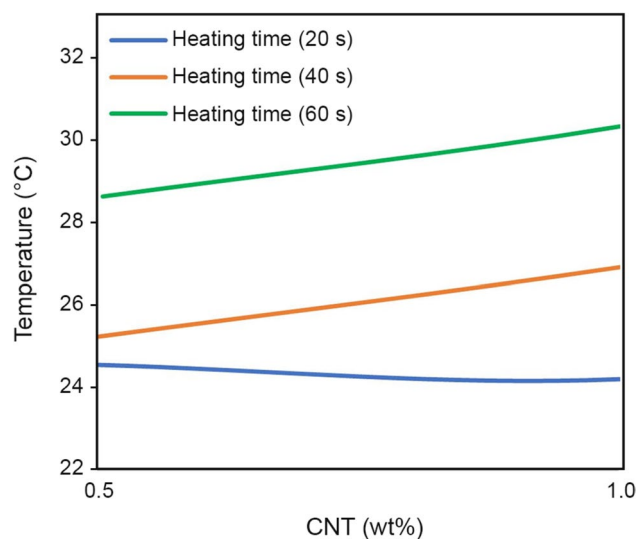


**Fig. 13** Temperature alterations of PP, and PP/CNT composites for various durations

characteristics of the composites compared to pristine PP, underscoring the impact of CNT fillers on the dimensional stability of the materials. In summary, our study provides valuable insights into the dimensional stability and thermal behavior of PP/CNT composites. The results underscore the pivotal roles played by the interaction between CNTs and the PP matrix, along with the strong interface between the nanotubes and polymer chains, in enhancing dimensional stability and reducing shrinkage. These findings hold significance for applications requiring materials with improved thermal stability and dimensional performance, particularly in high-temperature environments [28–30].

Figures 13 and 14 illustrate the temperature variations of pure PP and its composites over different durations. In the experiments involving PP/CNT composites, it is observed that beyond 20 s of heating, the temperature of composites with 0.5% and 1.0% (by weight) CNT content begins to rise. This temperature escalation is attributed to the presence of CNTs, which augment heat transfer and enhance thermal conductivity compared to pristine PP. The temperature increase becomes more pronounced with higher CNT content, signifying improved heat dissipation and enhanced thermal conductivity within the nanocomposite system. Similarly, experiments employing microwave heating on nanocomposites with varying MWCNT percentages reveal a continuous and noticeable increase in temperature with higher MWCNT content. This observation underscores the influence of MWCNTs in augmenting the heat absorption and conversion properties of nanocomposites under microwave irradiation. The heating efficiency, as represented by the slope of the temperature curves, also exhibits an upward trend with increasing MWCNT loading, indicating enhanced

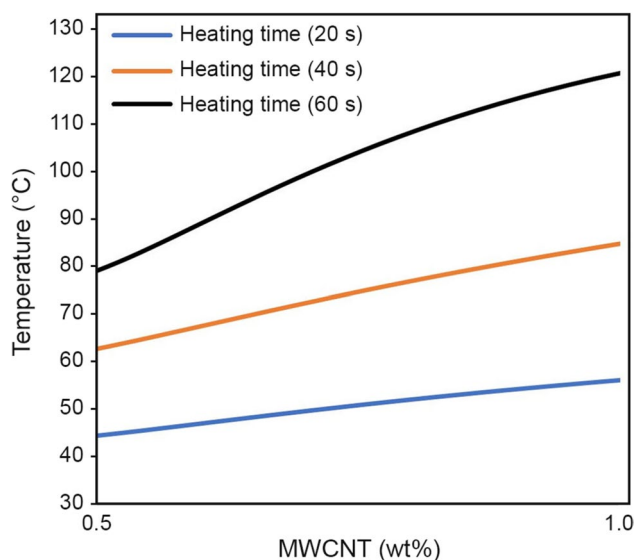


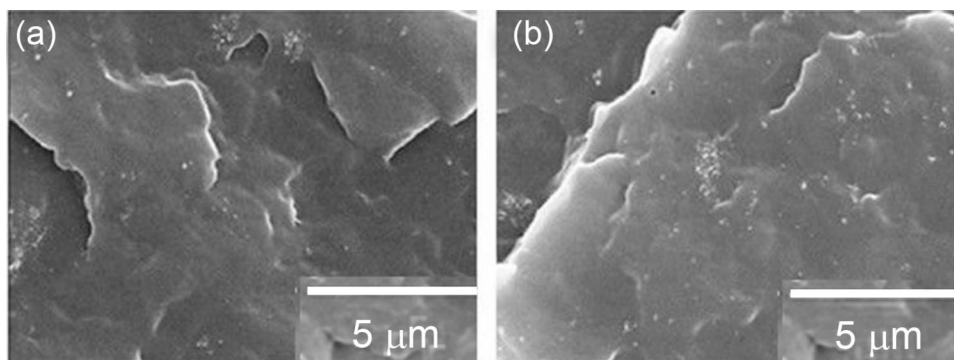
**Fig. 14** Temperature alterations of PP, and PP/MWCNT composites for various durations

heating capability. The correlation between MWCNT content and heating efficiency provides valuable insights into the microwave heating behavior of the nanocomposites, suggesting a pivotal role of MWCNTs in facilitating the absorption and conversion of microwave energy into heat, thereby improving heating performance [37–39]. The optimal content of MWCNTs for microwave susceptor applications is determined to be 1.0% (by weight), ensuring high uniformity of heating and minimizing the occurrence of hot spots that could disrupt the heating process. Quantitatively comparing the data, in experiments involving heating time, the temperature rises in PP/CNT composites (0.5% and 1.0% by weight) is observed after 20 s, indicating a delayed thermal response compared to pristine PP. Conversely, in microwave heating experiments, the temperature increase in nanocomposites is directly proportional to the MWCNT content, showing a continuous rise as the percentage of MWCNTs increases. The slope of the temperature curves, representing heating efficiency, also demonstrates an increasing trend with

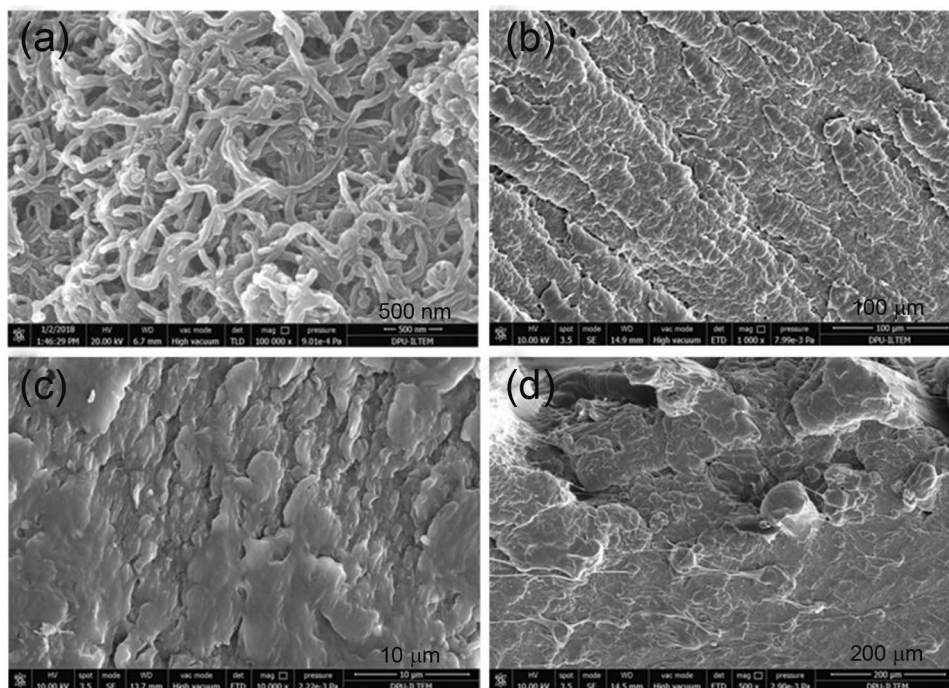
higher MWCNT loading, indicating a more pronounced temperature rise per percentage of MWCNT. In summary, the incorporation of CNTs in both heating methods enhances the thermal properties and heating efficiency of the composites. Although PP/CNT composites exhibit delayed temperature response under prolonged heating, they demonstrate improved heat dissipation and thermal conductivity. In microwave heating, nanocomposites with higher MWCNT loading exhibit enhanced heat absorption and conversion, resulting in greater temperature increases and heating efficiency [34–36].

Figure 15a and b showcase SEM images illustrating PP/CNT composites with varying CNT concentrations (0.5% and 1.0% by weight). Similarly, Fig. 16a–d depict SEM images presenting MWCNTs, PP, and PP composites with distinct MWCNT contents (0.5% and 1.0% by weight), respectively. The SEM visuals reveal that CNTs up to a concentration of 1.0% (by weight) are uniformly distributed throughout the PP matrix, indicating successful dispersion at lower CNT loadings and a homogeneous distribution within the composite material. However, achieving enhanced dispersion and a more uniform distribution of CNTs in the nanocomposites may necessitate further optimization of processing conditions. SEM analysis plays a crucial role in assessing the dispersion of nanofillers within a polymer matrix and understanding their reinforcing properties. It offers a macroscopic view of the sample surface, enabling the observation of overall nanofiller distribution and agglomeration. SEM images in Fig. 12c and d reveal that while some individual MWCNTs are dispersed throughout the PP matrix in the 0.5% and 1.0% (by weight) PP/MWCNT nanocomposites, there are areas where the nanotubes are not fully dispersed [42–44]. This underscores the need for continued efforts to improve dispersion and achieve a more uniform distribution of MWCNTs. In comparison, SEM analysis of the PP/CNT composites aligns with the quantitative data discussed earlier. The results indicate that as the CNT percentage increases (from 0.5 to 1.0% by weight), there is a further substantial temperature rise in the PP/CNT composites, signifying improved heat dissipation and thermal

**Fig. 15** SEM images of PP/CNT composites with various CNT contents of: **a** 0.5% (by weight), and **b** 1.0% (by weight)



**Fig. 16** SEM images of: **a** MWCNT, **b** PP, **c** PP/MWCNT 0.5% (by weight), and **d** PP/MWCNT 1.0% (by weight)



conductivity. Similarly, in the SEM images, the 1.0% (by weight) filled PP/MWCNT nanocomposite exhibits a higher dispersion of individual MWCNTs and fewer agglomerates compared to the 0.5% (by weight) sample. This suggests that a higher CNT content enhances dispersion and ensures a more uniform distribution of nanotubes within the composite material. To summarize, SEM analysis verifies the successful dispersion of CNTs in the PP matrix at lower loadings and provides visual evidence of nanotube distribution and agglomeration. However, additional optimization is warranted to achieve enhanced dispersion and a more uniform distribution of CNTs in the nanocomposites. The SEM results correlated with the quantitative data, affirming that a higher CNT content leads to improved dispersion and a more pronounced temperature rise in the PP/CNT composites [40–42].

Figures 17 and 18 present XRD images illustrating the crystalline structure of PP/CNT composites, pure PP, and PP/MWCNT composites, respectively. These XRD tests were conducted to investigate the crystalline structure and crystallization behavior of both pure PP and PP/MWCNT composites. In Fig. 17, the XRD test results for PP composites with 0.5% and 1.0% (by weight) CNT content reveal that the presence of CNTs acts as restriction sites, impeding the highly ordered spherulite formation of PP segments. Although CNTs were present, no discernible alterations in the PP crystal structure were observed. The predominant crystalline form of PP was found to be monoclinic ( $\alpha$ -form). Understanding the mechanical behavior of these composites hinges on discerning how the addition of CNTs has altered

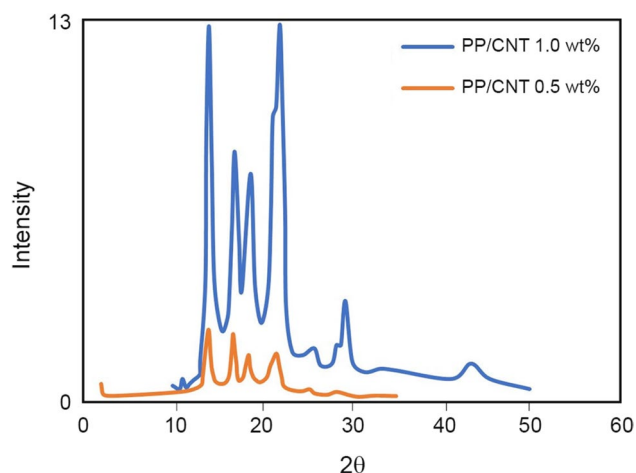


**Fig. 17** XRD of PP/CNT composites

the crystallization process of PP [48]. Moving to Fig. 18, the XRD patterns reveal the influence of MWCNTs on the crystal structure and properties of the composite material. Changes in peak intensity and width in the diffraction patterns indicate the impact of MWCNTs on the crystalline structure of PP. Notably, the XRD analysis did not show the presence of the  $\alpha$ -crystal form in both PP and PP/MWCNT composites. Instead, the addition of MWCNTs promoted the formation of the  $\beta$ -crystalline phase, suggesting potential enhancements in mechanical properties, thermal stability, and reinforcement of the composite. These findings provide valuable insights for the design and optimization of

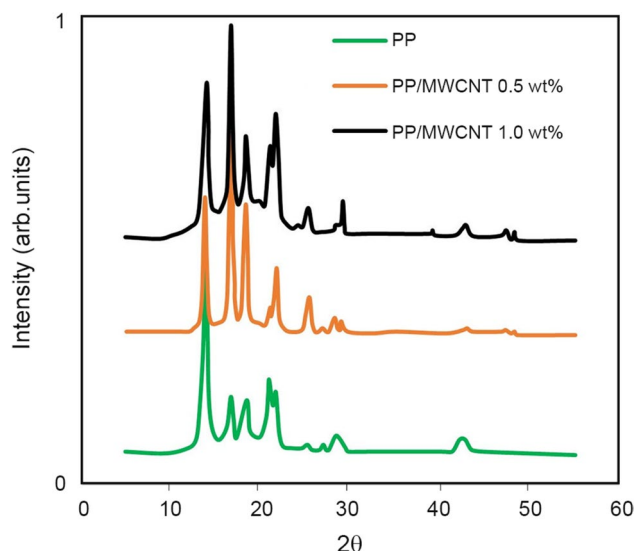


Fig. 18 XRD of PP, and PP/MWCNT composites

PP/MWCNT composites tailored for specific applications. In summary, the XRD test results highlight the influence of MWCNTs on the crystalline structure of PP/MWCNT composites, emphasizing the promotion of the  $\beta$ -crystalline phase. This addition has the potential to improve the mechanical properties and thermal stability of the composite, paving the way for the development of new composite materials with enhanced performance [45–47].

Figures 19 and 20 present the Raman spectra of PP/CNTs composites, MWCNT, and PP/MWCNT composites, respectively. These figures offer insights into the graphitization of CNTs or MWCNTs and their dispersion within polymers, shedding light on their interactions with the PP

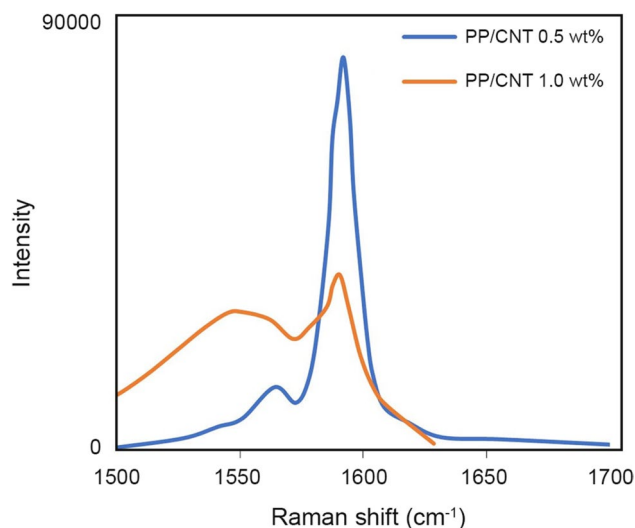


Fig. 19 Raman intensity of PP/CNTs composites

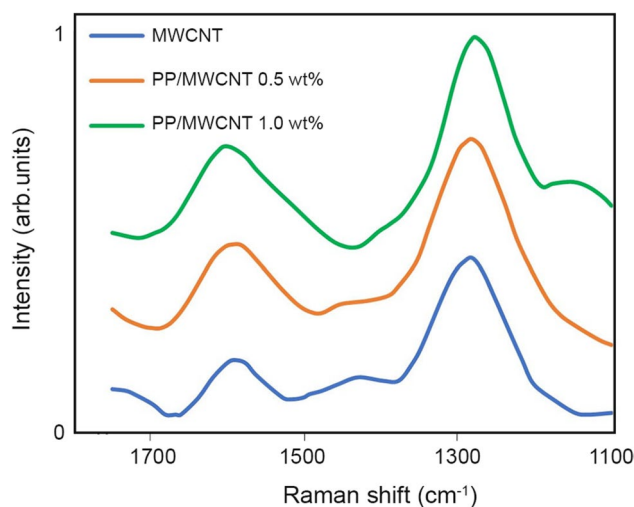


Fig. 20 Raman intensity of MWCNT and PP/MWCNT composites

matrix. In the Raman spectra of PP/MWCNT composites, distinct characteristics, such as the G band and the D band, become evident, indicating the graphitic structure of the nanotubes. Notably, sharp peaks within the spectral ranges of  $1205\text{--}1710\text{ cm}^{-1}$  and  $145\text{--}205\text{ cm}^{-1}$  are observable in the Raman spectra of PP/CNT composites. The upshift observed in the G band signals an increase in nanotube concentration within the polymer matrix. This upshift is attributed to the enhanced dispersion and alignment of nanotubes, potentially contributing to improved mechanical, electrical, or thermal properties of the composite material [50]. The utilization of nucleating agents can further amplify this effect by promoting crystallization and providing sites for crystal growth, as evidenced in DSC tests. It is crucial to acknowledge that specific details and mechanisms may vary based on the nanotube-polymer system. Therefore, additional experimental studies are imperative to comprehensively understand the reasons behind the observed upshift of the G band. Conversely, the Raman spectrum of PP composites with 0.5% and 1.0% (by weight) CNT or MWCNTs content reveals characteristic peaks associated with the presence of defects or carbonaceous compounds (D band) and the stretching of the C–C bond (G band). The intensity of the G band is closely linked to the dispersion of CNTs or MWCNTs, with an increase that may indicate improved dispersion. In summary, Raman spectroscopy provides valuable insights into the graphitic structure, dispersion, and alignment of CNTs or MWCNTs within PP matrices. The observed upshift of the G band in the Raman spectrum signifies improved dispersion and alignment of nanotubes, which holds the potential to enhance the properties of the composite material [49].



## Conclusion

The study focused on investigating the effects of incorporating both CNTs and MWCNTs into the PP matrix, aiming to elucidate their influence on various properties of the resulting nanocomposites. Through rigorous analysis, it was observed that the introduction of CNTs and MWCNTs significantly impacted the crystallization behavior, mechanical characteristics, thermal stability, and thermal shrinkage of the composite materials. Specifically, the addition of CNTs and MWCNTs was found to elevate the critical cooling rate for PP crystallization and increase the crystallization temperature during cooling. Isothermal crystallization tests highlighted the role of CNTs in expediting the development of the  $\alpha$ -phase crystalline structure, demonstrating their nucleation efficiency within the PP matrix. Moreover, the dynamic mechanical analysis revealed a notable enhancement in the storage modulus, signifying the reinforcing effect induced by CNTs. Interestingly, in hot air aging studies, composites containing CNTs exhibited more significant degradation compared to control samples, indicating potential trade-offs in certain environmental conditions. Additionally, the investigation into the thermal behavior of PP nanocomposites with MWCNTs revealed evidence of interactions between PP and the composites, leading to reduced thermal shrinkage. These comprehensive findings emphasize the multifaceted impacts of CNTs and MWCNTs on the mechanical, thermal, and crystallization properties of the composite materials. In conclusion, the study underscores the potential of PP/MWCNT nanocomposites, particularly in applications requiring enhanced thermal properties and increased interfacial area. The findings provide valuable insights into the complex interplay between nanotube fillers and the PP matrix, paving the way for tailored material design and optimization for specific application demands.

**Acknowledgements** The author extends sincere gratitude to Dr. Hassan Soleimani for his invaluable guidance and expertise throughout the course of this study. Additionally, acknowledgment is given to the Material Science Laboratory of Universiti Teknologi Petronas for providing essential facilities and resources that played a crucial role in the successful execution of this research.

**Author contributions** UTB conceptualized and conducted the analysis. The practical experiments were exclusively carried out at the Material Nanoscience Center at UTP.

**Data availability** Data availability is provided as requested from corresponding author.

**Code availability** On the author's request, readers can view and download the data needed to duplicate or further analyze the findings reported in the paper.

## Declarations

**Conflict of interest** The authors declare no conflicts of interest that could potentially influence or bias the submitted work.

**Ethical approval** As this study did not involve any living organisms, ethical approval was not required.

## References

1. Asgary AR, Nourbakhsh A, Kohantorabi M (2013) Old newsprint/polypropylene nanocomposites using carbon nanotube: preparation and characterization. *Compos B* 45:1414–1419
2. Huang J, Rodrigue D (2014) The effect of carbon nanotube orientation and content on the mechanical properties of polypropylene-based composites. *Mater Des* 55:653–663
3. Karsli NG, Yesil S, Aytac A (2014) Effect of hybrid carbon nanotube/short glass fiber reinforcement on the properties of polypropylene composites. *Compos B* 63:154–160
4. Ameli A, Nofar M, Park CB, Tschke PP, Rizvi G (2014) Polypropylene/carbon nanotube nano/microcellular structures with high dielectric permittivity, low dielectric loss, and low percolation threshold. *Carbon* 71:206–217
5. Felicia S, Laurentiu SI, Catalin F (2014) Effect of processing parameters and strain rate on mechanical properties of carbon nanotube-filled polypropylene nanocomposites. *Compos B* 59:109–122
6. Das D, Satapathy BK (2014) Designing tough and fracture-resistant polypropylene/multi-wall carbon nanotubes nanocomposites by controlling stereo-complexity and dispersion morphology. *Mater Des* 54:712–726
7. Huang G, Wang S, Song P, Wu C, Chen S, Wang X (2014) Combination effect of carbon nanotubes with graphene on intumescent flame-retardant polypropylene nanocomposites. *Compos A* 59:18–25
8. Daugaard AE, Jankova K, Hvilsted S (2014) Poly(lauryl acrylate) and poly(stearyl acrylate) grafted multiwalled carbon nanotubes for polypropylene composites. *Polymer* 55:481–487
9. Das D, Satapathy BK (2014) Microstructure-rheological percolation-mechanical properties correlation of melt-processed polypropylene-multiwall carbon nanotube nanocomposites: Influence of matrix tacticity combination. *Mater Chem Phys* 147:127–140
10. Chen L, Tang CY, Ku HSL, Tsui CP, Chen X (2014) Microwave sintering and characterization of polypropylene/multi-walled carbon nanotube/hydroxyapatite composites. *Compos B* 56:504–511
11. Gong J, Fen J, Liu J, Jiang Z, Chen X, Mijowska E, Wen X, Tang T (2014) Catalytic carbonization of polypropylene into cup-stacked carbon nanotubes with high performances in adsorption of heavy metallic ions and organic dyes. *Chem Eng J* 248:27–40
12. Mohammed HAS (2015) Electrically conductive carbon nanotube/polypropylene nanocomposite with improved mechanical properties. *Mater Des* 85:76–81
13. Rahmanian S, Suraya AR, Othman RN, Zahari R, Zainudin ES (2015) Growth of carbon nanotubes on silica microparticles and their effects on mechanical properties of polypropylene nanocomposites. *Mater Des* 69:181–189
14. Patti A, Barretta R, Marotti FS, Mensitieri G, Menna C, Russo P (2015) Flexural properties of multi-wall carbon nanotube/polypropylene composites: experimental investigation and nonlocal modeling. *Compos Struct* 131:282–289
15. Nair ST, Vijayan PP, Xavier P, Bose S, Soney CG, Thomas S (2015) Selective localization of multi-walled carbon nanotubes



- in polypropylene/natural rubber blends to reduce the percolation threshold. *Compos Sci Technol* 116:9–17
16. Liang JZ, Chen CY, Zou SY, Tsui CP, Tang CY, Zhang SD (2015) Melt flow behavior of polypropylene composites filled with multi-walled carbon nanotubes during extrusion. *Polym Test* 45:41–46
  17. Wan F, Tran MP, Leblanc C, Béchet E, Plougonven E, Léonard A, Detrembleur C, Noels L, Thomassi JM, Nguyen VD (2015) Experimental and computational micro-mechanical investigations of compressive properties of polypropylene/multi-walled carbon nanotubes nanocomposite foams. *Mech Mater* 91:95–118
  18. Djoudi H, Gelin JC, Barrière T (2015) Experiments and FE simulation for twin screw mixing of nanocomposite of polypropylene/multi-walled carbon nanotubes. *Compos Sci Technol* 107:169–176
  19. Lin JY, Wang WY, Chou SW (2015) Flexible carbon nanotube/polypropylene composite plate decorated with poly(3,4-ethylenedioxythiophene) as efficient counter electrodes for dye-sensitized solar cells. *J Power Sources* 282:348–357
  20. Galindo B, Benedito A, Gimenez E, Compan V (2016) Comparative study between the microwave heating efficiency of carbon nanotubes versus multilayer graphene in polypropylene nanocomposites. *Compos B* 98:330–338
  21. Verma P, Verma M, Gupta A, Chauhan SS, Malik RS, Choudhary V (2016) Multi-walled carbon nanotubes induced viscoelastic response of polypropylene copolymer nanocomposites: effect of filler loading on rheological percolation. *Polym Test* 55:1–9
  22. Liang JZ, Zhou TY, Zou SY (2016) Non-isothermal crystallization properties of polypropylene composites filled with multi-walled carbon nanotubes. *Polym Test* 55:184–189
  23. Wang PH, Ghoshal S, Gulgunje P, Verghese N, Kumar S (2016) Polypropylene nanocomposites with polymer-coated multiwall carbon nanotubes. *Polymer* 100:244–258
  24. Ghoshal S, Wang PH, Gulgunje P, Verghese N, Kumar S (2016) High impact strength polypropylene containing carbon nanotubes. *Polymer* 100:259–274
  25. Zhong J, Isayev AI, Zhang X (2016) Ultrasonic twin screw compounding of polypropylene with carbon nanotubes, graphene nanoplates and carbon black. *Eur Polym J* 80:16–39
  26. Li G, Hu C, Zhai W, Zhao S, Zheng G, Dai K, Liu C, Shen C (2016) Particle size-induced tunable positive temperature coefficient characteristics in electrically conductive carbon nanotubes/polypropylene composites. *Mater Lett* 182:314–317
  27. Lin JH, Lin ZI, Pan YJ, Hsieh CT, Lee MC, Lou CW (2016) Manufacturing techniques and property evaluations of conductive composite yarns coated with polypropylene and multi-walled carbon nanotubes. *Compos A* 84:354–363
  28. Wu K, Xue Y, Yang W, Chai S, Chen F, Fu Q (2016) Largely enhanced thermal and electrical conductivity via constructing double percolated filler network in polypropylene/expanded graphite e Multi-wall carbon nanotubes ternary composites. *Compos Sci Technol* 130:28–35
  29. Rosehr A, Luinstra GA (2017) Polypropylene composites with finely dispersed multi-walled carbon nanotubes covered with an aluminum oxide shell. *Polymer* 120:164–175
  30. Kazemi Y, Kakroodi AR, Wang S, Ameli A, Filleter T, Potschke P, Park CB (2017) Conductive network formation and destruction in polypropylene/carbon nanotube composites via crystal control using supercritical carbon dioxide. *Polymer* 129:179–188
  31. Joa SJ, Yua MH, Kimb WS, Kim HS (2018) Damage detection and self-healing of carbon fiber polypropylene (CFPP)/carbon nanotube (CNT) nanocomposite via addressable conducting network. *Compos Sci Technol* 167:62–70
  32. Wallner GM, Grabmanna MK, Klocker C, Buchberger W, Nitsche D (2018) Effect of carbon nanotubes on the global aging behavior of  $\beta$ -nucleated polypropylene random copolymers for absorbers of solar-thermal collectors. *Sol Energy* 172:141–145
  33. Wang PH, Sarkar S, Gulgunje P, Verghese N, Kumar S (2018) Structure and rheological behavior of polypropylene interphase at high carbon nanotube concentration. *Polymer* 150:10–25
  34. Liang JZ, Zou SY, Du Q (2018) Impact and flexural properties of polypropylene composites reinforced with multi-walled carbon nanotubes. *Polym Test* 70:434–440
  35. Wang PH, Sarkar S, Gulgunje P, Verghese N, Kumar S (2018) Fracture mechanism of high impact strength polypropylene containing carbon nanotubes. *Polymer* 151:287–298
  36. Anjali S, Aishwaryalakshmi S, Ashwin V, Neeraja S, Rasana N, Jayanarayanan K (2018) Effect of compatibilizer and carbon nanotubes on blends of polypropylene and Nylon 6. *Mater Today Proc* 5:25524–25533
  37. Liu YF, Feng LM, Chen YF, Shi YD, Chen XD, Wang M (2018) Segregated polypropylene/cross-linked poly(ethylene-co-1-octene)/multi-walled carbon nanotube nanocomposites with low percolation threshold and dominated negative temperature coefficient effect: towards electromagnetic interference shielding and thermistors. *Compos Sci Technol* 159:152–161
  38. Yetgin SH (2019) Effect of multi-walled carbon nanotube on mechanical, thermal, and rheological properties of polypropylene. *J Mater Res Technol* 8:4725–4735
  39. Hu Y, Li D, Wu L, Yang J, Jian X, Bin Y (2019) Carbon nanotube bucky paper and buckypaper/polypropylene composites for high shielding effectiveness and absorption-dominated shielding material. *Compos Sci Technol* 181:107699
  40. Qi XD, Sun DX, Yang CJ, Wang WY, Wang Y (2019) Synergistic toughening of carbon nanotubes and nucleating agent in polypropylene/ethylene-propylene-diene terpolymer blend. *Polym Test* 75:185–191
  41. Sruthi S, Abhilash R, Tharun K, Krishna PG, Jayanarayanan K, Rasana N (2020) Experimental and theoretical investigation on the non-isothermal crystallisation kinetics of polypropylene reinforced with multiwalled carbon nanotubes. *Mater Today Proc* 33:2264–2273
  42. Liu Z, Li L, Zheng G, Liu C, Mi L, Li Q, Liu X (2020) Effect of small amount of multi-walled carbon nanotubes on crystallisation and thermal-mechanical properties of overflow micro-injection molded isotactic polypropylene. *Compos Commun* 21:100381
  43. Patil J, Sankpal R, Rathod D, Patil K, Kubade PR, Kulkarni HB (2021) Studies on mechanical and thermal performance of carbon nanotubes/polypropylene nanocomposites. *Mater Today Proc* 46:7182–7186
  44. Kim GM, Kil T, Lee HK (2021) A novel physicomechanical approach to dispersion of carbon nanotubes in polypropylene composites. *Compos Struct* 258:113377
  45. Nuaklong P, Boonchoo N, Jongvivatsakul P, Charinpanitkul T, Sukontasukkul P (2021) Hybrid effect of carbon nanotubes and polypropylene fibers on mechanical properties and fire resistance of cement mortar. *Constr Build Mater* 275:122189
  46. Graves KA, Higgins LJR, Nahil MA, Mishra B, Williams PT (2022) Structural comparison of multi-walled carbon nanotubes produced from polypropylene and polystyrene waste plastics. *J Anal Appl Pyrolysis (JAAP)* 161:105396
  47. Smith JA, Johnson MB, Thompson LG (2020) Investigating the impact of multiwalled carbon nanotubes on the mechanical and thermal properties of polypropylene-based composites. *Polym Compos* 41:4562–4573
  48. Chen Y, Wang H, Liu Q (2021) Enhancing the flame-retardant properties of polypropylene using a combination of carbon nanotubes and graphene oxide. *J Fire Sci* 39:256–271
  49. Rodriguez A, Martinez B, Gonzalez C (2021) Synergistic effects of carbon nanotubes and nanoclay on the electrical conductivity and flame resistance of polypropylene nanocomposites. *Polym DegradStab* 183:109403

50. Wu Z, Li Y, Zhang H (2022) Tailoring the mechanical performance of polypropylene through the addition of functionalized multiwalled carbon nanotubes. *J Appl Polym Sci* 139:50945

author(s) or other rightsholder(s); author self-archiving of the accepted manuscript version of this article is solely governed by the terms of such publishing agreement and applicable law.

Springer Nature or its licensor (e.g. a society or other partner) holds exclusive rights to this article under a publishing agreement with the